

Quantum skyrmions and the destruction of long-range antiferromagnetic order in the high- T_c superconductors $\text{La}_{2-x}\text{Sr}_x\text{CuO}_4$ and $\text{YBa}_2\text{Cu}_3\text{O}_{6+x}$

Eduardo C. Marino and Marcello B. Silva Neto

Instituto de Física, Universidade Federal do Rio de Janeiro, Caixa Postal 68528, Rio de Janeiro - RJ, 21945-970, Brazil

(December 2, 2024)

We study the destruction of the long range antiferromagnetic order in the high- T_c superconductors $\text{La}_{2-x}\text{Sr}_x\text{CuO}_4$ and $\text{YBa}_2\text{Cu}_3\text{O}_{6+x}$ in the framework of the CP^1 -nonlinear sigma model formulation of the two-dimensional quantum Heisenberg antiferromagnet. The dopants are introduced as independent fermions with appropriate dispersion relations determined by the shape of the Fermi surface. The energy of skyrmion topological defects, which are shown to be introduced by doping, is used as an order parameter for the antiferromagnetic order. We obtain analytic expressions for this as a function of doping which allow us to plot the curves $T_N(x_c) \times x_c$ and $M(x)/M(0) \times x$, for both YBCO and LSCO, in good quantitative agreement with the experimental data.

PACS number(s): 74.72.Bk, 74.25.Ha

High-temperature superconductivity is by now well established to arise from doping quasi two-dimensional (quasi-2D) Mott-Hubbard antiferromagnetic insulators. The doping process initially produces the destruction of the antiferromagnetic ordering, giving place to a quantum spin-liquid disordered phase [1]. The two best studied examples are $\text{La}_{2-x}\text{Sr}_x\text{CuO}_4$ (LSCO) and $\text{YBa}_2\text{Cu}_3\text{O}_{6+x}$ (YBCO) for which the Néel ordered ground state at $x = 0$ [2] is replaced by a quantum disordered state for $x_c \approx 0.02$ [3] and $x_c \approx 0.41$ [4], respectively.

It has long been recognized that the pure compounds are well described in terms of a $S = 1/2$ quantum Heisenberg antiferromagnet (QHAF) on a square lattice. The long wavelength spin fluctuations of the latter, on the other hand, are described by the $O(3)$ quantum nonlinear sigma model (QNL σ M) in two space plus one time dimension [5,6] whose Lagrangian density is

$$\mathcal{L} = \frac{\rho_s}{2} \left[\frac{1}{c^2} (\partial_\tau \mathbf{n})^2 + (\nabla \mathbf{n})^2 \right], \quad (1)$$

with the constraint $\mathbf{n}^2 = 1$, where \mathbf{n} is the order parameter field and ρ_s and c are respectively the spin-stiffness and spin-wave velocity.

The nonlinear sigma model possesses classical topologically nontrivial solutions called *skyrmions* whose energy is $E_s = 4\pi\rho_s$. For fully quantized skyrmions, on the other hand, there is a reduction of the skyrmion energy to half of the above classical value [7]

$$E_s = 2\pi\rho_s. \quad (2)$$

Having in mind that the skyrmion energy is reduced by quantum fluctuations, it is natural to expect it to be further reduced by the extra fluctuations introduced through doping. Furthermore, since in the framework of the NL σ M the skyrmion energy is proportional to the

ground state magnetization we can use it as an order parameter for the quantum phase transition which leads to the destruction of the antiferromagnetic state.

In this paper, we revisit the continuum model proposed in [8], to describe the doping process in $\text{YBa}_2\text{Cu}_3\text{O}_{6+x}$ (YBCO) at $T = 0$, and extend it for including also the case of LSCO. The model predicts the creation of skyrmion topological defects precisely at the dopant's positions, as has been proposed earlier [9]. The presence of these disorder the system, thereby reducing the ground state magnetization. As a consequence, the skyrmion energy itself is lowered and eventually vanishes at the Néel quantum critical point. By computing quantum defect correlation functions at $T = 0$, we obtain analytical expressions for the skyrmion energy as a function of doping, $E_s(x)$, which allow us to plot the curves $M(x) \times x$. Subsequently, introducing finite temperature and interlayer coupling we obtain the antiferromagnetic part of the phase diagram, namely the curve $T_N(x_c) \times x_c$, for both LSCO and YBCO, in good quantitative agreement with experiment. As we shall see, our analysis is compatible with a picture in which the formation of stripes would occur in LSCO but not in YBCO.

The doping process: The chemical modification of parent compounds of high- T_c materials produces the introduction of holes in the Oxygen orbitals in the layered CuO_2 planes. In what follows, we shall determine how the skyrmion energy is modified by the presence of such holes. To this end we propose that the doped system can be described in terms of a bulk ($T = 0$) $O(3)$ QNL σ M coupled to four-component fermion fields whose dispersion relation is determined by the shape of the Fermi surface. These represent the holes doped into the in-plane O^{--} orbitals, whereas the nonlinear sigma field represents the spin density of the active electrons of the Cu^{++} ions. For describing the coupling of the dopants to the

Cu^{++} spins, it will be convenient to make use of the CP^1 language, where $\mathbf{n} = z_i^\dagger \sigma_{ij} z_j$ with σ_{ij} being the Pauli matrices and z_i^\dagger, z are complex scalar fields. Then, following [8], we minimally couple the fermions to the CP^1 fields. This is consistent with previous results where a minimal coupling of fermions to CP^1 fields was obtained in the long wavelength regime of the spin-fermion model [10]. Finally, the fermion dispersion relation, obtained by expanding the energy around the Fermi surface, will depend on the compound under consideration and for this reason we have to treat each case separately.

a) For YBCO we have an almost circular shape for the Fermi surface [11] and for this reason we shall use the dispersion relation $\epsilon(k) = \sqrt{k^2 v_F^2 + (m^* v_F^2)^2}$, with m^* and v_F being respectively the effective mass and Fermi velocity of the dopants, see Fig. 1a. The doped system can then be described by the partition function

$$\begin{aligned} \mathcal{Z} = & \int \mathcal{D}[\bar{z}, z, \mathcal{A}_\mu, \bar{\psi}, \psi] \delta[\bar{z}z - 1] \delta[j^\mu - \Delta^\mu] \\ & \times \exp \left\{ \int_0^\infty d\tau \int d^2\mathbf{x} [2\rho_s (D_\mu z_i)^\dagger (D^\mu z_i) \right. \\ & \left. + \bar{\psi} (i\partial - \frac{m^* v_F}{\hbar} - \gamma^\mu \mathcal{A}_\mu) \psi + \mathcal{L}_H] \right\} \end{aligned} \quad (3)$$

where we allow for a Hopf term $\mathcal{L}_H = (\theta/2) \epsilon^{\mu\alpha\beta} \mathcal{A}_\mu \partial_\alpha \mathcal{A}_\beta$, which must appear in the presence of topological defects on the ground state [12]. As usual, $D_\mu = \partial_\mu + i\mathcal{A}_\mu$, with $\partial_\mu = (\partial_\tau/c, \nabla)$, and $\mathcal{A}_\mu = iz_i^\dagger \partial z_i$ is the Hubbard-Stratonovich CP^1 vector field.

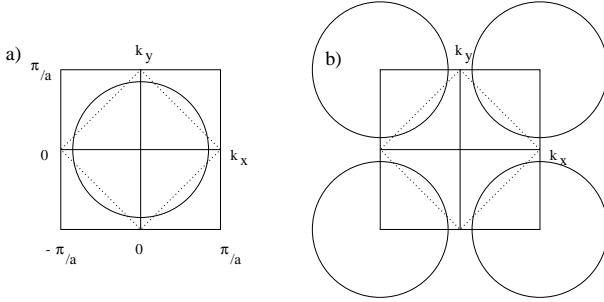


FIG. 1. Approximate Fermi surfaces for: a) $\text{YBa}_2\text{Cu}_3\text{O}_{6+x}$ and b) $\text{La}_{2-x}\text{Sr}_x\text{CuO}_4$ [11].

The second delta functional constraint in (3) is used in order to introduce the in-plane hole concentration parameter δ . In its argument, $j^\mu = \bar{\psi} \gamma^\mu \psi$ and $\Delta^\mu = 4\delta \int_{X,L}^\infty d\xi^\mu \delta^3(z - \xi)$ for a dopant introduced at the position X and moving along the line L . The factor of four in the definition of Δ^μ accounts for the degeneracy of the representation of the Fermi fields. The zeroth component of the associated Lagrange multiplier will be the chemical potential. Similarly to what has been shown in [8], upon integration over the fields $\bar{z}, z, \bar{\psi}, \psi$, the resulting equation of motion for \mathcal{A}_0 is such that a skyrmion topological defect configuration concides with the dopant position at

any time and $\pi\theta = 2\delta$. In other words, holes dress with skyrmions. This justifies our inclusion of the Hopf term in (3) for nonzero doping. We stress that, because of the CP^1 constraint, there is a mass term for the \mathcal{A}_μ field. As a consequence, there will be neither statistical transmutation nor the generation of spurious in-plane magnetic fields [8] which would be inconsistent with muon spin relaxation (μSR) experiments [13].

The parameter δ counts the density of holes in the CuO_2 planes. This must be connected to the oxygen stoichiometry parameter x . For YBCO, it is known that the out of plane chains play an important role in the process of doping. At low doping, $x \leq 0.18$ for instance, most of the holes go to the out of plane O-Cu-O chains and the system can be considered as pure. In view of this we propose that the density of in-plane charge carriers is related to the oxygen stoichiometry by $\delta = x - 0.18$.

In order to study the destruction of the Néel state, as announced, we shall use the fact that the skyrmion energy E_s is an order parameter for antiferromagnetism. For evaluating E_s , we observe that skyrmions are topological defects whose quantum properties can be fully described by disorder field operators μ [14]. Using these, we calculate the large distance behavior of the skyrmion correlation function, $\langle \mu^\dagger(X) \mu(Y) \rangle \rightarrow e^{-\frac{E_s}{\hbar c} |X - Y|} / |X - Y|^\nu$, from which we can obtain the skyrmion energy E_s [7]. For the pure system we have that E_s is given by (2). For the partition function (3), we obtain, after integration over \bar{z}, z , and $\bar{\psi}, \psi$ fields, that [8]

$$E_s(\delta) = 2\pi\rho_s \left(1 - \frac{\gamma\hbar c}{\pi a_D \rho_s} \delta^2 \right), \quad (4)$$

where $\gamma = \frac{32\pi(9\pi^2 - 16)}{(\pi^2 + 16)^2} = 10.9398$ is a numerical factor that comes from the integration over the fermions, and $a_D \equiv a/\sqrt{2} = 2.68 \text{ \AA}$, the minimal distance between two oxygen atoms, is the lattice spacing for dopants. The above skyrmion energy can be put in the form $E_s = 2\pi\rho_s(\delta)$ if we define an effective δ dependent spin-stiffness

$$\rho_s(\delta) = \rho_s \left(1 - \frac{\gamma\hbar c}{\pi a_D \rho_s} \delta^2 \right). \quad (5)$$

We then conclude, after comparing (4) with (2), that the doped system can be described by a QNL σ M with a generalized δ dependent spin-stiffness given by (5).

To check the above statement we must look at the behaviour of the reduced sublattice magnetization as a function of doping $M(x)/M(0) = \sqrt{\rho_s(x)/\rho_s}$, see Fig. 2. We see that our theoretical prediction is in good agreement with experiment and $\rho_s(\delta)$ vanishes for

$$\delta_c = \sqrt{\frac{\pi\rho_s a_D}{\gamma\hbar c}}. \quad (6)$$

For $\hbar c = 1.0 \text{ eV \AA}$ and $\rho_s = 0.069 \text{ eV}$ we obtain $\delta_c = 0.23 \pm 0.03$ or $x_c = 0.41 \pm 0.03$ for the quantum critical point.

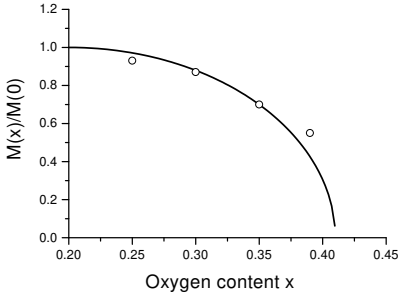


FIG. 2. Reduced sublattice magnetization $M(x)/M(0) = \sqrt{\rho_s(x)/\rho_s}$ for $\text{YBa}_2\text{Cu}_3\text{O}_{6+x}$. Experimental data from [15].

b) For LSCO, on the other hand, the Fermi surface is given approximately by the one of Fig. 1b, which has also been observed in angle-resolved photoemission spectroscopy (ARPES) [16]. We now observe that the Fermi surface of LSCO can be obtained by shifting the one of YBCO towards $(\pi/a, \pi/a)$ and symmetry related points in the Brillouin zone. This leads to the new dispersion relation $\epsilon(k) = \sqrt{[(k_x \pm \pi/a)^2 + (k_y \pm \pi/a)^2]v_F^2 + (m^*v_F^2)^2}$, which corresponds to a kinetic term for the fermions in (3) modified by a shifted derivative term. Even though the partition function remains unchanged, this shift will have a non-trivial effect on the skyrmion correlation function and energy because of the constraint on the fermionic density of states. The computation of these proceeds as before [8,7] and we now obtain the following expression for the skyrmion energy

$$E_s(\delta) = 2\pi\rho_s \left(1 - \frac{\gamma\hbar c}{\pi a_D \rho_s} (4\delta)^2 - \frac{2\sqrt{2}\hbar c}{a\rho_s} (4\delta) \right). \quad (7)$$

There are two important differences between (7) and (4). The first one is a linear δ dependence in (7) which is absent in (4). This was generated by the shift in the dispersion relation and is a consequence of the fact that the Fermi surface of LSCO is not centered in the Brillouin zone. The second one is an extra factor of four multiplying δ in (7), which is needed to account for the four branches of the Fermi surface of this compound.

The above skyrmion energy suggests, in accordance to what has been done for the case of YBCO, that the doped system could presumably be described by a nonlinear sigma model with stiffness

$$\rho_s(\delta) = \rho_s \left(1 - \frac{\gamma\hbar c}{\pi a_D \rho_s} (4\delta)^2 - \frac{2\sqrt{2}\hbar c}{a\rho_s} (4\delta) \right). \quad (8)$$

However, we find that the corresponding reduced sublattice magnetization has a faster decrease with doping than the one observed by experiment, see solid line in Fig. 3. This can be interpreted as a signal of stripes formation in LSCO (see also [17]). In connection to this, we have

noticed that the correct experimental behavior can be reproduced if we assume that the δ dependent stiffness is conversely given by

$$\rho'_s(\delta) = \rho_s \sqrt{1 - \frac{\gamma\hbar c}{\pi a_D \rho_s} (4\delta)^2 - \frac{2\sqrt{2}\hbar c}{a\rho_s} (4\delta)}, \quad (9)$$

instead of (8). Now the corresponding sublattice magnetization agrees with the experimental data as can be seen from the dashed line in Fig. 3. Observe that for LSCO we have used the well known fact that $x = \delta$. Interestingly, the location of the quantum critical point apparently is not affected by the formation of stripes. In fact, both $\rho_s(\delta)$ and $\rho'_s(\delta)$ vanish at

$$\delta_c = \frac{1}{4} \frac{\sqrt{(2\sqrt{2}\hbar c/a)^2 + 4\gamma\hbar c\rho_s/\pi a_D} - (2\sqrt{2}\hbar c/a)}{2(\gamma\hbar c/\pi a_D)}. \quad (10)$$

For $\hbar c = 0.75$ eV Å and $\rho_s = 0.051$ eV Å we obtain $x_c = \delta_c = 0.020 \pm 0.003$ for the quantum critical point.

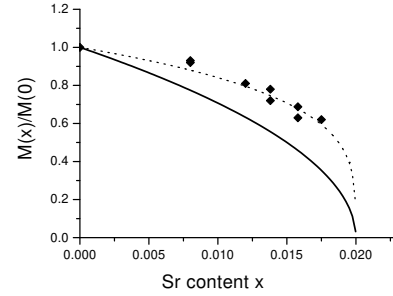


FIG. 3. Reduced sublattice magnetization for $\text{La}_{2-x}\text{Sr}_x\text{CuO}_4$. Experimental data from [3].

The phase diagram: In order to obtain the critical line of the $T_N \times x_c$ phase diagram we must consider a nonzero interlayer coupling J_\perp . For this purpose, we shall use the partition function [18]

$$\mathcal{Z} = \int \mathcal{D}\mathbf{n}_i \exp \left\{ -\frac{\rho_s}{2\hbar} \int_0^{\hbar\beta} d\tau \int d^2\mathbf{x} \sum_i \left[\frac{1}{c^2} (\partial_\tau \mathbf{n}_i)^2 + (\nabla \mathbf{n}_i)^2 + \alpha (\mathbf{n}_{i+1} - \mathbf{n}_i)^2 \right] \right\} \delta(\mathbf{n}_i^2 - 1), \quad (11)$$

where $\alpha = (1/a^2)J_\perp/J_{||}$, with J_\perp and $J_{||}$ being respectively the interlayer and intralayer couplings of the underlying microscopic lattice quasi-2D QHAF and $\beta = 1/T$ ($k_B = 1$). Contrary to the strictly 2D case now a finite value for the Néel temperature is obtained to order $1/N$ in a large N expansion [18]:

$$T_N = 4\pi\rho_s \left[\ln \left(\frac{2T_N^2}{\alpha(\hbar c)^2} \right) + 3 \ln \left(\frac{4\pi\rho_s}{T_N} \right) - 0.0660 \right]^{-1}. \quad (12)$$

Now, if we replace in (12) the spin-stiffness ρ_s by our δ dependent expressions (5) and (9), respectively for YBCO and LSCO, and using $J_\perp/J_{||} \simeq 5 \times 10^{-5}$, we obtain the phase diagrams plotted below.

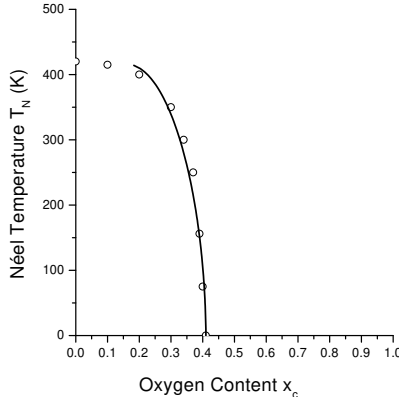


FIG. 4. Antiferromagnetic phase diagram for $\text{YBa}_2\text{Cu}_3\text{O}_{6+x}$, $T_N(x_c) \times x_c$. Experimental data from [4].

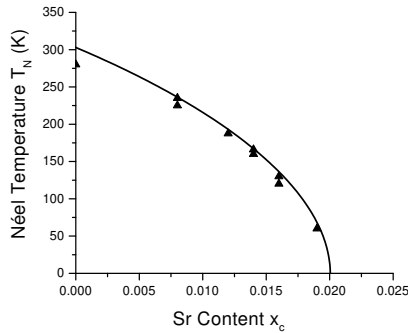


FIG. 5. Antiferromagnetic phase diagram for $\text{La}_{2-x}\text{Sr}_x\text{CuO}_4$. Experimental data from [3].

In summary, our results indicate that the antiferromagnetic phase of the high- T_c cuprates can be described in terms of a generalized $\text{NL}\sigma\text{M}$ with an effective, doping dependent, spin stiffness which carries all the information about the quantum fluctuations introduced by the dopants. Our results point towards a picture in which charged stripes presumably occur in LSCO, causing a slow down of the decrease of the sublattice magnetization as a function of doping in comparison to the case where they are absent, see Fig. 3. Apparently, the only effect of such phenomenon is to divide by two the quantum critical exponent of the spin stiffness, without affecting the location of the quantum critical point. At the present stage we still do not have a theoretical justification for such a change in the behavior of the spin stiffness with doping. This is an issue which deserves further investigation. Conversely, our results indicate that such phenomenon is absent in YBCO as our model (3)

was able to satisfactorily reproduce the zero temperature data for $M(x)/M(0)$, see Fig. 2. This is in agreement with density matrix renormalization group calculations in the context of the n -leg ladder $t - t' - J$ model [19].

As a final comment we would like to remark that for the case of $\text{Bi}_2\text{Sr}_2\text{CaCu}_2\text{O}_{8+x}$ we expect that our results shall reproduce the experimental data without the scaling modifications done for LSCO. Indeed this material, while having a Fermi surface similar to LSCO, does not seem to present the formation of stripes.

We are indebted to A. H. Castro Neto, A. A. Katanin, B. Koiller, C. Kübert and J. Schmalian for many useful comments. We also acknowledge P. Carretta for pointing out Ref. [15]. E.C.M. was partially supported by CNPq and FAPERJ. M.B.S.N was supported by FAPERJ.

- [1] P. W. Anderson, *Science* **235**, 1196 (1987).
- [2] B. Keimer *et al.*, *Phys. Rev. B* **45**, 7430 (1992).
- [3] F. Borsa *et al.*, *Phys. Rev. B* **52**, 7334 (1995).
- [4] J. Rossat-Mignod *et al.*, *Dynamics of Magnetic Fluctuations in High-Temperature Superconductors*, G. Reiter, P. Horsch and G. C. Psaltakis, Eds., Plenum, NY, 1991.
- [5] F. D. M. Haldane, *Phys. Rev. Lett.* **50**, 1153 (1983).
- [6] S. Chakravarty, B. I. Halperin and D. R. Nelson, *Phys. Rev. B* **39**, 2344 (1989).
- [7] E. C. Marino, *Phys. Rev. B* **61**, 1588 (2000).
- [8] E. C. Marino, *Phys. Lett. A* **263**, 446 (1999).
- [9] P. B. Wiegmann, *Phys. Rev. Lett.* **60**, 821 (1988).
- [10] C. Kübert and A. Muramatsu, *Phys. Rev. B* **47**, 787, 1993.
- [11] A. P. Kampf, *Phys. Rep.* **249**, 219 (1994).
- [12] F. D. M. Haldane, *Phys. Rev. Lett.* **61**, 1029 (1988).
- [13] R. F. Kiefl *et al.*, *Phys. Rev. Lett.* **64**, 2082 (1990).
- [14] E. C. Marino, in *NATO ASI Series, Applications of Statistical and Field Theory Methods in Condensed Matter*, D. Baeriswyl, A. Bishop and J. Carmelo, Eds., Plenum, NY, (1990).
- [15] C. Bucci *et al.*, *Hyperfine Interactions* **105**, 71 (1997).
- [16] I. Ano *et al.*, *J. Phys. Soc. Jpn.* **68**, 1249 (1999).
- [17] A. H. Castro Neto and D. Hone, *Phys. Rev. Lett.* **76**, 2165 (1995).
- [18] V. Yu. Irkhin and A. A. Katanin, *Phys. Rev. B* **55**, 12318 (1997); *Phys. Rev. B* **57**, 379 (1998).
- [19] S. R. White and D. J. Scalapino, *Phys. Rev. Lett.* **80**, 1272 (1998); *Phys. Rev. Lett.* **81**, 3227 (1998).